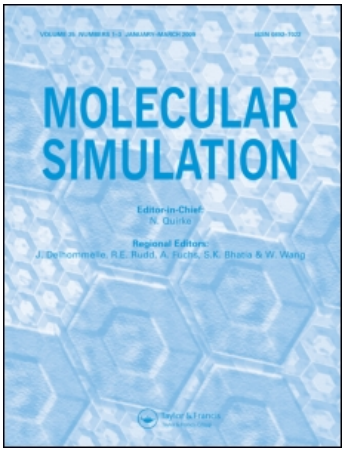

Molecular Simulation
Publication details, including instructions for authors and subscription information:
http://www.informaworld.com/smpp/title~content=t713644482

Kinetics of Adsorption of *n*-butane on an Aggregate of Silicalite by Transient Non-equilibrium Molecular Dynamics

J. M. Simon[a]; A. Decrette[a]; J. B. Bellat[a]; J. M. Salazar[a]
[a] Laboratoire de Recherches sur la Reactivite des Solides, UMR 5613 du CNRS, Universite de Bourgogne, Dijon Cedex, France

To cite this Article Simon, J. M. , Decrette, A. , Bellat, J. B. and Salazar, J. M.(2004) 'Kinetics of Adsorption of *n*-butane on an Aggregate of Silicalite by Transient Non-equilibrium Molecular Dynamics', Molecular Simulation, 30: 9, 621 — 629
To link to this Article: DOI: 10.1080/08927020410001717254
URL: http://dx.doi.org/10.1080/08927020410001717254

Molecular Simulation, VOL. 30 (9), 10 August 2004, pp. 621–629

Taylor & Francis
Taylor & Francis Group

Kinetics of Adsorption of *n*-butane on an Aggregate of Silicalite by Transient Non-equilibrium Molecular Dynamics

J.M. SIMON*, A. DECRETTE, J.B. BELLAT and J.M. SALAZAR

Laboratoire de Recherches sur la Reactivite des Solides, UMR 5613 du CNRS, Universite de Bourgogne, BP 47870, 21078 Dijon Cedex, France

(Received January 2004; In final form April 2004)

Here we present the results obtained by using a transient non-equilibrium molecular dynamics procedure (TNEMD) which allows us to study the kinetics of gas adsorption at different gas pressures. Our simulations were focused on the adsorption of *n*-butane on aggregates of silicalite at 300 K. These simulations give relevant information on both the equilibrium state and the kinetics of adsorption. The isotherms obtained are in agreement with previous experimental and simulated results. At the equilibrium state our simulations allowed us to identify five energetic sites on the aggregate: three inside the micropores (straight and zig-zag channels and their intersections) and two additional ones at the external surface. Moreover, our simulations show, as determined exprimentally, that the *n*-butane is adsorbed on the external sites of the zeolite only at high filling (high loadings) of the zeolite—i.e. close to the saturation. From the simulated kinetics we calculated the Fick's diffusion coefficients at different loadings.

Keywords: Zeolite; Silicalite; Adsorption; *n*-Butane; Isotherm and kinetics of adsorption; Molecular simulation

INTRODUCTION

Zeolites are a class of nanoporous minerals with a crystalline structure. The shape of the porosity and the chemical nature of these minerals give to them specific properties of adsorption [1,2]. In this paper, we focus on the silicalite which is a pure siliceous MFI zeolite ($[SiO_2]_{96}$ per unit cell) [2] characterized by interconnected straight and zig-zag channels. It is well known that this zeolite is hydrophobic and organophilic. For these reasons oil companies use it in catalytic cracking processes [3,4]. Moreover, given its shape selectivity they are good candidates to be used in the separation of *n* iso-paraffins. Among the several mechanisms governing the separation, the kinetics of adsorption is a key process. This kinetics depends on three factors: the gas diffusion, the intercrystalline diffusion (diffusion between the zeolite grains) and the intracrystalline diffusion (diffusion in the micropores). Generally, the first two factors are neglected because they are supposed to be faster than the third one, which is assumed to be the limiting step. The diffusion coefficient of the adsorbate in the zeolite can be determined by different techniques. One approach is based on transient macroscopic experiments (gravimetry, manometry and chromatography) which gives the Fick's diffusion coefficients. Other techniques are pulse field gradient nuclear magnetic resonance (PFG-NMR) and quasi elastic neutron scattering (QENS). These two last techniques allow us to study the mobility of the adsorbed molecules at the microscopic (equilibrium) level and they give the self diffusion coefficients. The link between the self diffusion coefficients and the Fick's diffusion coefficients is detailed by Krishna *et al.* [5]. However, the diffusion coefficients obtained by microscopic and macroscopic approaches differ by several orders of magnitude [6,7]. These differences are usually explained by the influence of the crystalline defects of the zeolite (e.g. polycrystalline aggregates, macro and mesoporosity, blocked pores, partially coating or/and amorphization of the external surface, hydroxyl groups) and by the resistance to the mass transfer through the external surface.

Since a decade ago many authors studied the transport properties of adsorbed alkanes molecules into zeolites by using molecular dynamics (MD)

*Corresponding author. E-mail: jean-marc.simon@u-bourgogne.fr

ISSN 0892-7022 print/ISSN 1029-0435 online © 2004 Taylor & Francis Ltd
DOI: 10.1080/08927020410001717254

simulations at equilibrium [8]. In general these simulations are performed by using as an initial state an equilibrium configuration generated by grand canonical Monte-Carlo simulations (GCMC) including configurational bias. These MD-simulations give the self diffusion coefficients by means of Einstein's relation [8,9]. Other simulation techniques, used for slow molecules, are based on the rare events methods [10], like for instance the transition path sampling. The self diffusion coefficients obtained by these techniques are qualitatively in agreement with the experimental microscopic results. However, these simulations do not provide any information concerning the mass transfer from the gaseous phase to the adsorbed phase and cannot give any insight about the discrepancy between microscopic and macroscopic diffusion coefficients obtained experimentally.

To gain a physical understanding on the global kinetics a few authors have recently used realistic Non-Equilibrium Molecular Dynamics (NEMD) to study directly the permeation across the zeolites [11,12]. The method consists of a simulation box containing a zeolite, adsorbed molecules and two buffer regions used to create a gradient (by inserting and/or removing molecules) of chemical potential. Some authors consider the buffer regions in the most external parts of the zeolites while others consider the buffer regions as a gas phase. Moreover, the initial configurations are generated by GCMC and the evolution is tracked by means of MD and GCMC. In other words the evolution is followed by a given number of MD steps and then new molecules are inserted and/or removed by a GCMC step. This allows us to have a non-equilibrium steady state which can be used to calculate the Onsager's coefficients [13], L, by means of the relations fluxes (J)–thermodynamic forces ($\nabla\mu$): $J = -L\nabla\mu$, with μ the chemical potential of the adsorbed phase.

Even when these approaches allow us to study non steady states regimes, as far as we know, these regimes have not been yet investigated. Here, we will enterprise an analysis of these regimes by means of an approach similar to those mentioned above but differing on the initial configuration state and on the way the dynamics are generated. That is to say, here we do not use a buffer region but instead the simulation box contains a zeolite surrounded by a gas phase with a fixed number of particles, and the dynamics are generated exclusively by MD simulations. This procedure, which we will call transient non-equilibrium molecular dynamics (TNEMD), presents the advantage that we can access to the transient adsorption behavior at different gas pressures and determine the Fick's diffusion coefficient in analogy with experiments (manometric). Namely, we are interested in simulating the adsorption kinetics of *n*-alkanes on aggregates of silicalite.

The paper presented here is organized in the following way: the models and the interaction potentials we used for the silicalite and for the *n*-butane are presented in the second section, and the simulation method and computational details are described in the third section. Finally in the fourth section, we present and discuss the results obtained.

MODEL

The ideal silicalite aggregate (without defects) was simulated by using a flexible atomic model [14] with 18 unit cells (1728 atoms of silicon and 3456 atoms of oxygen) and with an orthorhombic Pnma crystallographic structure [15]. By taking the crystallographic parameters $a = 20.022\,\text{Å}$, $b = 19.899\,\text{Å}$, $c = 13.383\,\text{Å}$, with b the direction of the straight channels, the dimensions of the aggregate were $L_a = 3_a$, $L_b = 2b$ and $L_c = 3c$. The initial atomic positions were determined from crystallographic experimental data [15]. In this zeolite representation, given that neither hydrogen nor hydroxyl groups were added to the external surface, the atomic coordinance of the zeolite at this surface was not correct. Here, we assumed that these defects will have a minor role on the kinetics of adsorption of *n*-butane. Moreover, due to the zeolite construction, the structure of the aggregate external surfaces depends on their orientations. The external surfaces perpendicular to the a and c directions ([1 0 0] and [0 0 1]) exhibited half straight channels, with the pores opening at the bottom of the half channels. The two external surfaces perpendicular to the b direction [0 1 0] were flat with the pores emerging at the surfaces.

The molecules of *n*-butane were modeled by using the united atoms (UA) model proposed by Ryckaert and Bellemans [16]. Each methyl (CH_3) and methylene (CH_2) group was simulated as one center of force. The dynamics of the atoms (silicalite and *n*-butane) were governed by inter- and intramolecular interaction potentials.

The site–site intermolecular interaction is given by a truncated Lennard-Jones potential:

$$V_{\text{LJ}}(r_{ij}) = \begin{cases} 4\epsilon_{ij}\left[\left(\frac{\sigma_{ij}}{r_{ij}}\right)^{12} - \left(\frac{\sigma_{ij}}{r_{ij}}\right)^{6}\right], & r_{ij} < r_c \\ 0, & r_{ij} \geq r_c \end{cases} \quad (1)$$

where r_c is the potential cut-off radius, r_{ij} the distance between sites i and j and σ_{ij} and ϵ_{ij} are the potential parameters. We used the Lorentz-Berthelot mixing rules to determine the potential parameters for unlike site interactions: $\epsilon_{ij} = (\epsilon_{ii}\epsilon_{jj})^{1/2}$ and $\sigma_{ij} = (\sigma_{ii} + \sigma_{jj})/2$ where ϵ_{ii} and σ_{ii} are the potential parameters for like site interactions. In our simulations, we fixed

$r_c = 2.5\,\sigma_{Si}$ where σ_{Si} is the potential parameter of silicon.

The intramolecular potential energy includes; bond, angle, torsion and coupling terms. The former of these potentials is harmonic

$$V_S(r_i) = \frac{1}{2}k_s(r_i - r_0)^2, \tag{2}$$

where k_s is the stretching force constant, r_0 is the equilibrium bond length, and r_i is the instantaneous bond length. The angle bending potential we used here is given by

$$V_B(\beta_i) = \frac{1}{2}k_\beta(\beta_i - \beta_0)^2, \tag{3}$$

with k_β the bending force constant, β_0 the equilibrium bond angle, and β_i the instantaneous bond angle. For the *n*-butane we used a torsion potential given by a third order polynomial:

$$V_T(\phi_i) = \sum_{i=0}^{3} a_i(\cos\phi_i)^i, \tag{4}$$

where ϕ_i is the torsional angle.

In our simulations, we used a coupling between a stretching and bending, a stretching–stretching and bending–bending vibration modes. For this we proceed as suggested by Ermoshin *et al.* [14] and the coupling potentials we used are the following:

$$V_{SB}(r_i, \beta_i) = k_{s\beta}(r_i - r_0)(\beta_i - \beta_0), \tag{5}$$

with $k_{s\beta}$ the stretching–bending coupling force constant.

$$V_{SS}(r_i, r_j) = k_{ss}(r_i - r_0)(r_j - r_0), \tag{6}$$

where k_{ss} was the stretching–stretching coupling force constant between i and j,

$$V_{BB}(\beta_i, \beta_j) = k_{\beta\beta}(\beta_i - \beta_0)(\beta_j - \beta_0), \tag{7}$$

with $k_{\beta\beta}$ the bending–bending coupling force constant between angles i and j. In Table I, we summarize the values we used in our simulations for the interaction potentials.

TABLE I The model and potential data. The parameters of the *n*-butane molecules are taken from Ref. [17]

Mass of the interacting sites (kg mol^{-1}):		
$m_{CH_2} = 0.014026$ $m_{CH_3} = 0.015034$		
$m_O = 0.0159994$ $m_{si} = 0.028086$		
Lennard-Jones	ϵ/R/K	σ/Å
CH_2	47.00	3.930
CH_3	98.10	3.770
Si	82.3777	3.9598
O	29.4257	3.06221
Stretching	r_0/Å	k_s/(kJ mol^{-1})
CC	1.523	2649.7
SiO	1.59	3239.86
Bending	β_0	k_b/(kJ mol^{-1})
CCC	113.0°	519.64625
OsiO	109.5°	469.72
SiOSi	149°	72.2646
Coupling stretching	Stretching	k_{ss}/(kJ mol^{-1})
SiO	Si common	114.419
SiO	O common	150.55
Coupling bending	Stretching	$k_{s\beta}$/(kJ mol^{-1})
OsiO	SiO common	78.286
OsiO	Si common	−78.286
Coupling bending	Bending	$k_{\beta\beta}$/(kJ mol^{-1})
OsiO	SiO common	−66.242
OsiO	Si common	−192.705
Torsion /kJ mol^{-1}:		
$a_0 = 8.395222$ $a_1 = 16.782046$		
$a_2 = 1.133585$ $a_3 = -26.310895$		

For the zeolite we used the parameters given by Ermoshin *et al.* [14], for the intramolecular potential and by Smirnov *et al.*, [18] for the Lennard-Jones parameters (R is the perfect gas constant).

SIMULATION DETAILS

Simulated Systems

The aggregate of silicalite and the gas of *n*-butane, before being in contact, are first stabilized independently at the same temperature (300 K). The initial configuration of the simulated system consists of a cubic simulation box (with periodic boundary conditions) with the zeolite at its center and the zeolite surrounded by N_{mol}^{add} molecules of *n*-butane which have been distributed randomly (Fig. 1). Initially, the zeolite is empty and the configuration settings described here have been used to study the kinetics of adsorption at different fillings. For avoiding molecules overlapping, we define an excluded volume around each molecule of gas. The volume of the cubic simulation box, V_{tot}, is given by the initial gas density, ρ_i, and in our simulations we used different densities ranging from 0.2 to 9.2 kg/m^3. Another interesting point is to study the adsorption kinetics on the zeolite initially containing a given amount of adsorbate. For this, we added N_{mol}^{add} molecules to the simulation box already containing N_{mol}^{init} molecules of *n*-butane. The total number of simulated molecules of *n*-butane, N_{mol}^{tol}, was then the sum of N_{mol}^{init} and N_{mol}^{add}. In Table II, we give the details of the configurations used in our simulations.

TNEMD

As mentioned in the introduction, the studies on the kinetics of adsorption by MD simulations are focused on the knowledge of the dynamical properties of the adsorbed phase [8]. Some authors calculate the intracrystalline diffusion coefficients (self diffusion coefficient or Fick's diffusion coefficient) at equilibrium which in most cases agree qualitatively with microscopic experiments (QENS and PFG-NMR) [6,7].

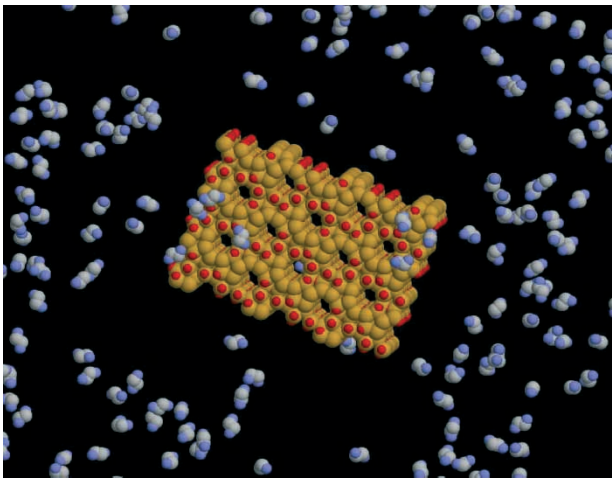

FIGURE 1 The initial configuration of an empty aggregate of silicalite surrounded by a gas of *n*-butane composed of 250 molecules, case 1 of Table II. In blue the pseudo atoms of methyl, in grey the methylens, in yellow the atoms of silicon and in red the oxygens (*b* axis is perpendicular to the plane sheet). In the plane of the figure, we can distinguish the straight channels of the zeolite. (Colour version available online.)

However, these results disagree with the diffusion coefficients determined from the adsorption kinetics of macroscopic experiments, like for instance manometric experiments. This last approach is based on a transient non-equilibrium regime [19] where, basically, the gas and the zeolite are brought in contact into a closed vessel where the pressure is measured. The gas is then adsorbed and the difference between the current pressure and the initial one is related to the amount of adsorbed gas. The generated kinetics is analyzed to determine the Fick's diffusion coefficient [6]. As far as we know, the specific transient regime observed by manometric experiments has not yet been investigated by MD simulations. In order to study this issue, we simulated the dynamics of a silicalite aggregate and a gas of *n*-butane for which we calculated the zeolite filling with time. By doing this, our simulations reproduce a transient non-equilibrium condition and for this reason we call this procedure transient non-equilibrium molecular dynamics simulation (TNEMD).

TABLE II The simulation conditions

Sim. no:	L_{tot}/Å	N_{mol}^{tot}	N_{mol}^{init}	N_{mol}^{add}
1	163.995	250	0	250
2	163.995	140	120	20
3	163.995	120	100	20
4	163.995	100	80	20
5	163.995	100	0	100
6	122.133	100	0	100
7	101.793	100	0	100
8	163.995	80	60	20
9	163.995	60	40	20
10	163.995	60	0	60
11	163.995	40	20	20
12	163.995	20	0	20
13	163.995	10	0	10

L_{tot} is the dimension of the edge of the simulation box, N_{mol}^{tot}, N_{mol}^{init} and N_{mol}^{add} are, respectively, the total number of molecules of *n*-butane included in the simulation box, the number of molecules in the gas phase and adsorbed in the zeolite at the initial equilibrium state and the number of *n*-butane added in the gas phase to this initial equilibrium state.

To obtain the system dynamics, we proceed by integrating the Newton's equations of motion by using the well known velocity Verlet algorithm [20]. The trajectories were generated by 3×10^6 simulation steps and by using a time step of 1 fs and the molecular dynamics procedure used guarantees the conservation of total energy and momentum. However, when a molecule of gas is adsorbed by the silicalite the potential energy decreases while the kinetic energy increases, and this may lead us to obtain large fluctuations of the system temperature. To overcome this difficulty, we applied a thermostat at the boundaries of the simulation box by rescaling the gas molecules velocities. That is to say, each time a gas molecule reaches a boundary of the simulation box we measured its temperature and if this was different from 300 K, we rescaled its velocity to have the desired temperature. We prefer to use this thermostat instead of the Nosé-Hoover thermostat [20,21] because we choose to work with a fixed temperature at the boundaries and not with a thermostat implying a relaxation delay, which is the case of the later thermostat. Our velocity rescaling implies a perturbation of the trajectories of the gas molecule but given that the boundaries are far enough from the surface of the aggregate (more than 40 Å), we can reasonably assume that the gas molecules have enough time to relax before being in contact with the zeolite and, therefore, these perturbations should have a minor impact on the adsorption kinetics. Given that our simulations are situated at the nanometric scale, the results of the kinetics are closely related to the initial configuration and so the statistical uncertainty of the computed diffusion coefficient is important. To have better statistics of the adsorption kinetics, we performed five different simulations for each simulated state (Table II) and the analytical properties were averaged over these simulations.

Thermodynamics Properties

Temperature Calculation

In our studies, the kinetic temperature, *T*, was obtained by combining two definitions of the internal kinetic energy, *K*, one coming directly from the equipartition of the energy and the second obtained from the kinetic contribution of the simulated particules;

$$K = \frac{1}{2}(3N_{at} - 6)k_B T = \frac{1}{2}\sum_{i=1}^{N_{at}} m_i \langle |\mathbf{v}_i - \mathbf{v}|^2 \rangle, \qquad (8)$$

at the left hand side of this equation N_{at} is the total number of atoms of the system, $3N_{at} - 6$ is total number of degrees of freedom of the system, k_B was the Boltzmann constant and T the temperature. At the right hand side, $\mathbf{v}_i$ is the instantaneous velocity of the atom i and mass m_i, and $\mathbf{v}$ is the barycentric instantaneous velocity.

Pressure Calculation

The gas pressure, P, was obtained by using the well known perfect gas law:

$$PV_{gas} = (N_{mol}^{tot} - N_{mol}^{ads})k_B T, \quad (9)$$

where N_{mol}^{ads} was the total number of molecules adsorbed, V_{zeo} the volume of the aggregate and $V_{gas} = V_{tot} - V_{zeo}$.

Filling of the Zeolite

The number of adsorption sites (i.e. straight, zig-zag channels and their intersections) per unit cell in the silicalite is equal to 12 in the bulk system (216 sites for 18 unit cells). In our aggregate, several sites are located at the external surface and the total number of intracrystalline adsorption sites is reduced to 144. To obtain the number of adsorbed molecules per unit cell, i.e. the loading θ, we divide the number of adsorbed molecules inside the pores by the number of intracrystalline sites in our aggregate (144 sites) and the resulting number was multiplied by the number of adsorption sites per unit cell in the silicalite (12 sites). To count the number of adsorbed molecules inside the zeolite during the simulation we used an energetic criteria which is described below.

RESULTS

In this section, we will first determine the equilibrium properties of the system; the adsorption isotherms and the most energetic adsorption sites of the silicalite at the interior of the pores and at the external surface, and these will be compared with results arising from other simulations and experiments. In the literature several authors [12,22] have already identified these adsorption sites for molecules of *n*-butane at the interior of the silicalite but given that in most of these simulations they consider an infinite silicalite, due to the use of periodic boundary conditions, the presence of an external surface is usually ignored. However, in a real situation a silicalite presents an external surface and for this reason we were interested in studying the influence of this surface on the adsorption kinetics. This issue will be helpful in understanding the passage from the gaseous phase to the adsorbed phase. The second part of our analysis will be focused on the adsorption kinetics which allowed us to determine the Fick's diffusion coefficients at different gas densities and fillings of the zeolite.

Equilibrium

In our simulation, we distinguished between the equilibrium state and the transient period (i.e. the passage from the initial configuration to the equilibrium state). The transient period was used to calculate the Fick's diffusion coefficient. In Fig. 2, we plotted the evolution of the number of adsorbed molecules in time, the uptake curve. In the first part of the curve the slope is positive and molecules of *n*-butane enter into the zeolite. When the maximum is reached the number of adsorbed molecules fluctuates around this maximum value and the numbers of molecules entering and leaving the zeolite are equal (Fig. 3); this corresponds to the equilibrium state.

The adsorption isotherm was calculated at 300 K by using the different simulation results at equilibrium. The values for the pressure ranged from 5 Pa to 8×10^4 Pa and they correspond to a loading of the zeolite from 0.8 to 11 molecules per unit cell. In Fig. 4, we compare our isotherm at 300 K with those obtained by experiments and by other simulations [17,23] at the same temperature. As one can see in the figure, each point of our isotherm is in agreement with other results.

To determine the different energetic adsorption sites, we plotted on Fig. 5 the histograms of the potential energy distribution between the zeolite and the *n*-butane for each point of the isotherm curve. Below 8.3 molecules per unit cell, there are two energetic sites corresponding to -63 and -55 kJ/mol, respectively. The height of these two picks increase in the same proportion as the loading

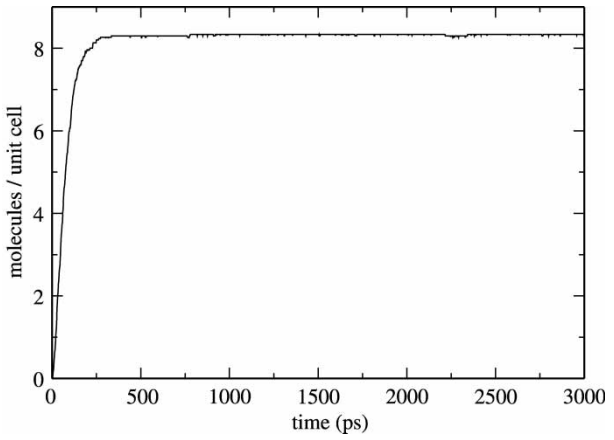

FIGURE 2 Kinetics of adsorption of 100 molecules of *n*-butane at 300 K, case 7 of Table II. The number of molecules adsorbed in the micropores is given in molecules per unit cell. The equilibrium state is reached after 400 ps, under equilibrium the loading θ slightly fluctuates around its averaged value, 8.1 molecules per unit cell.

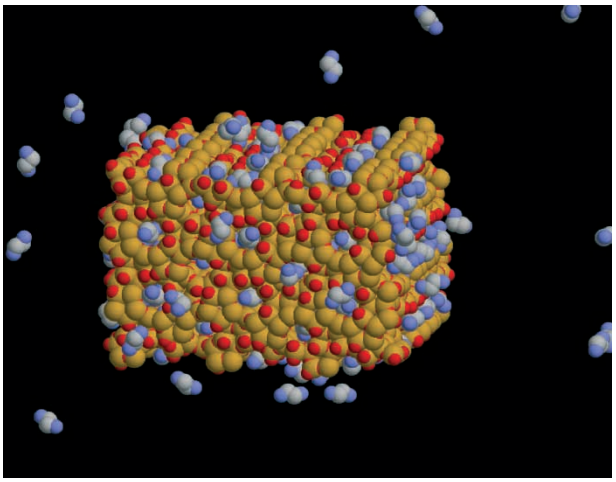

FIGURE 3 Equilibrium configuration of an aggregate of silicalite with 250 molecules of *n*-butane obtained by using the simulation procedure described in the "Simulation Details" section after a simulated trajectory of 3000 psec. The initial configuration leading to this equilibrium state corresponds to the case number 1 of Table II. In this figure, we used the same color code as in Fig. 1 (*b* axis is perpendicular to the plane sheet). The image clearly shows that part of the *n*-butane molecules have been adsorbed on the aggregate while the others remain in the gas phase. As we can see the adsorbed molecules are located inside the pores and on the external surface of the aggregate, mainly in the half straight channels. (Colour version available online.)

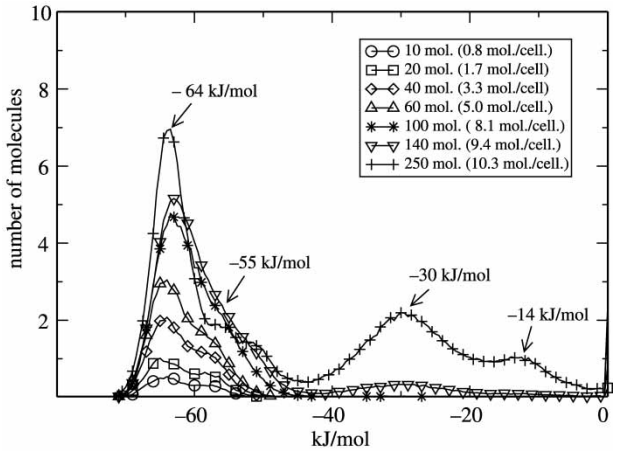

FIGURE 5 Histograms of the potential energy distribution between silicalite and molecules of *n*-butane at 300 K at different equilibrium loadings of the zeolite, in the range from 0.8 to 10.3 molecules per unit cell. At low loadings (below 8.3 molecules per unit cell) 2 picks emerge, one at −64 kJ/mol and the other one at −55 kJ/mol; at higher loadings, two additional (at −30 and −14 kJ/mol).

of the zeolite and their area ratio is a constant equal to 2. At higher loadings, two additional picks emerge at higher energies; one at −30 kJ/mol and the other one at −14 kJ/mol.

To localize the energetic sites of adsorption of the zeolite we plotted on Fig. 6 the profile of the interaction energy adsorbate–adsorbent along the [1 0 0] direction. The figure shows two energetic zones in the system; one zone at the external surfaces having two adsorption sites at −30 and −14 kJ/mol, respectively. The first one is located at a few angstroms inside the zeolite (in the bottom of the half straight channels) and the second located at the flat external surface of the zeolite (see Fig. 3). Therefore, it is not unphysical to suppose that these external adsorption sites will contribute to the adsorption kinetics (this issue will be discussed below). The second adsorption zone is inside the crystal and it is periodic. This periodicity can be associated with the straight, zig-zag channels and their intersections with energies −61, −64 and −55 kJ/mol, respectively. In our simulations, we

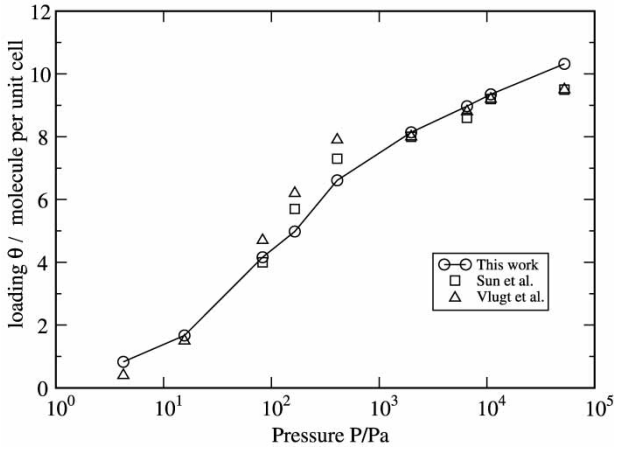

FIGURE 4 Comparison of the adsorption isotherms of *n*-butane on silicalite at 300 K obtained from experiments by Sun *et al.* [23], from the configurational-bias Monte Carlo simulations of Vlugt *et al.* [17], and from our MD simulations. The plot clearly shows a satisfactory agreement with all these isotherms.

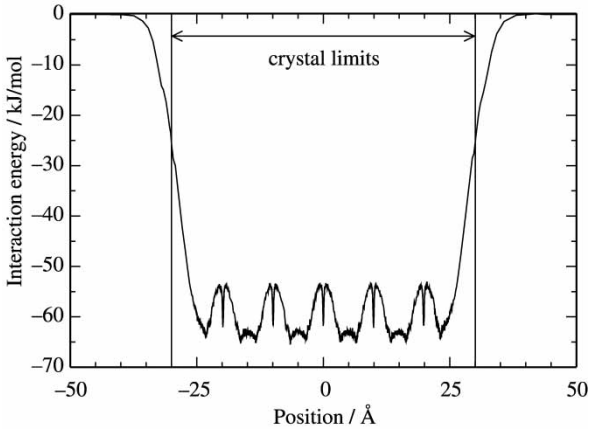

FIGURE 6 Profile of the potential energy between silicalite and molecules of *n*-butane at 300 K along the [1 0 0] crystallographic direction of the aggregate, case 1 of Table II. The crystallographic limits of the aggregate are shown on the figure. Inside the crystal, the profile of the energy is periodic, corresponding to the crystallographic periodicity of the straight and zig-zag channels and their intersections. At the external surfaces, the energy decreases from 0 to −45 kJ/mol and the curve presents two weak inflection points (at −14 and −30 kJ/mol); under those conditions, the height of the external surfaces is around 12 Å.

consider that a *n*-butane molecule is located inside the aggregate if its interaction energy with the zeolite is lower than $-45\,\mathrm{kJ/mol}$ and this constitutes the energetic criteria we used to count the number of adsorbed molecules inside the zeolite and for calculating the loading per unit cell, θ.

Kinetics of Adsorption

To better understand the role played by the external surfaces of the zeolite, we distinguished the adsorption kinetics of the molecules adsorbed on the aggregate from molecules adsorbed inside the pores. The former have an interaction potential energy with the zeolite which is lower than $-5\,\mathrm{kJ/mol}$ while the seconds have an interaction energy lower than $-45\,\mathrm{kJ/mol}$. These criteria imply two adsorption kinetics which we called global kinetics for the adsorbed molecules and intracrystalline kinetics for the molecules adsorbed inside the pores. To determine the Fick's diffusion coefficients we used the same protocol as in manometric experiments, i.e. we study the adsorption kinetics from the transient part of the uptake curves. The transient period, for long times, follows an exponential law. Usually, one assumes that the time necessary of a molecule to cross both the gas and the external surface is negligible compared with the adsorption kinetics. Under these conditions, the exponential parameter is directly related to the Fick's diffusion coefficient D [24] of the adsorbed phase:

$$N_{\mathrm{mol}}^{\mathrm{ads}}(\infty) - N_{\mathrm{mol}}^{\mathrm{ads}}(t) = A\exp(-\beta D t/(L_a^2 + L_b^2 + L_c^2)), \quad (10)$$

where $N_{mol}^{ads}(\infty)$ and $N_{mol}^{ads}(t)$ are the amount of molecules adsorbed on the aggregate (on the external surface and inside the pores) at equilibrium and at a given time t, respectively. Here t is the time spent from the beginning of the kinetics, A and β are constants that depend on the ratio between the final amount of gas and the final amount of adsorbed molecules.

The values of D which we call global diffusion coefficients are obtained from the global kinetics: its values are summarized in Table III for the simulations presented in Table II. The statistical errors are lower than ten per cent and we add in the Table III the values of the diffusion coefficients calculated from the adsorbed molecules inside the microporosity which we call D_{int} for intracrystalline diffusion coefficients. The values vary with the loading of the zeolite and they are ranged from 1×10^{-9} to $1 \times 10^{-8}\,\mathrm{m^2\,s^{-1}}$ and these agree qualitatively with previous results [7,9,25]. This suggests that the external surface does not play a role on the adsorption kinetics. To obtain accurate diffusion coefficients at different loadings, we increased by 20 molecules the density of the gas up to 140 molecules and by maintaining the volume of the simulation box constant (cases 2–4, 8, 9, 11 and 12). For each increase of molecules we calculated the diffusion coefficients. The calculated values, D and D_{int}, are given in Fig. 7. We also give in this figure the case of the lowest loading of the zeolite (see case 13 in Table II). Above 1 molecule per unit cell and below 7 molecules per unit cell the Fick's diffusion coefficients are rather constant. For higher (>7 molecules per unit cell) and lower (<1 molecule per unit cell) loadings, the diffusion coefficients are higher. For example, for a loading of 9.4 molecules per unit cell (140 molecules, case 2) and 5 molecules per unit cell (60 molecules, case 9), the ratio on the diffusion coefficients is a factor 2. For loadings below 8.3 molecules per unit cell, the obtained intracrystalline and global diffusion coefficients (see Fig. 7) are identical. Henceforth, under these conditions, we did not see any particular effect of the external surface of the aggregate on the kinetics of adsorption. However, at higher loadings the global kinetics is slower than the intracrystalline kinetics, for instance; at 10.3 molecules per unit cell (see case 1 of Table II) $D_{\mathrm{int}} \approx 2D$. As we mentioned in the last section, at these high loadings, molecules are trapped at equilibrium at the external energetic sites. The difference between these two diffusion coefficients is due to the fact that the adsorption kinetics on the external surface is balanced by an important desorption phenomena (in contrast with what occurs inside the nanopores). In consequence, this implies an increment of the time necessary to reach the equilibrium state at the external surface.

To have a better insight on the mobility of the adsorbed molecules and for avoiding the thermodynamic dependence of the diffusion coefficient with the loading of the zeolite, authors usually calculate the Maxwell Stefan's diffusion coefficients (D^{c} and $D_{\mathrm{int}}^{\mathrm{c}}$) instead of the Fick's diffusion

TABLE III Fick's diffusion coefficients of *n*-butane at 300 K calculated with Eq. (10) from the kinetics of intracrystalline adsorbed molecules D_{int} and from the global kinetics of adsorption D

Sim. no:	$D/(10^{-9}\,m^2\,s^{-1})$	$D_{int}/(10^{-9}\,m^2\,s^{-1})$
1	5.0	9.3
2	2.7	3.1
3	2.1	2.8
4	1.9	2.0
5	2.2	2.2
6	3.9	3.4
7	4.8	5.1
8	1.3	1.2
9	1.4	1.4
10	1.3	1.3
11	1.3	1.3
12	1.4	1.4
13	2.2	2.2

See Table II, to get the corresponding initial conditions used in the simulations.

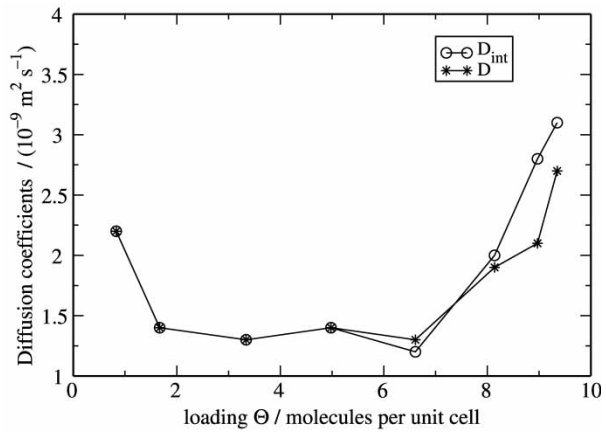

FIGURE 7 Comparison between the global (*) and intracrystalline (○) Fick's diffusion coefficients of *n*-butane at 300 K as a function of the loading of the zeolite calculated from the simulations corresponding to the initial cases 2–4, 8, 9, 11–13 of Table II. The two diffusion coefficients (D and D_{int}) are identical up to 8.3 molecules per unit cell (in the statistical uncertainty). For loadings higher than 8.3 molecules per unit cell the intracrystalline diffusion coefficients are higher. This can be associated with the adsorption on the external surface which have slower kinetics than the intracrystalline one.

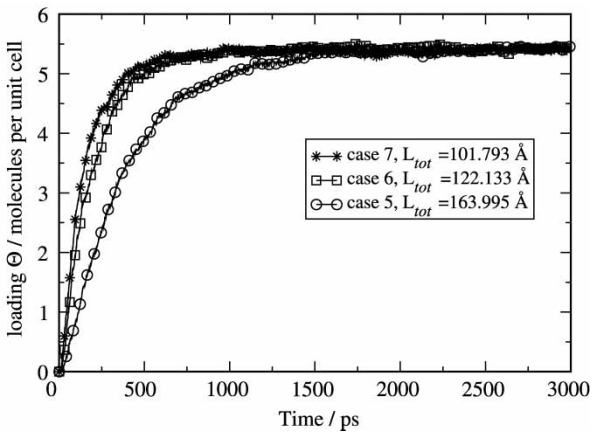

FIGURE 9 Here we show the effect of the density on the kinetics of adsorption of 100 molecules of *n*-butane at 300 K, cases 5–7 of Table II. This figure shows that the kinetics of adsorption decreases with the density of gas. The corresponding calculated diffusion coefficients (see Table III) decrease by more than a factor 2 between the kinetics of case 7 and 5.

coefficients. To obtain the former coefficients, the Fick's diffusion coefficients are corrected by a thermodynamic factor deduced from the isotherm:

$$D^{c} = D\frac{\mathrm{d}\ln(\theta)}{\mathrm{d}\ln(P)}.$$

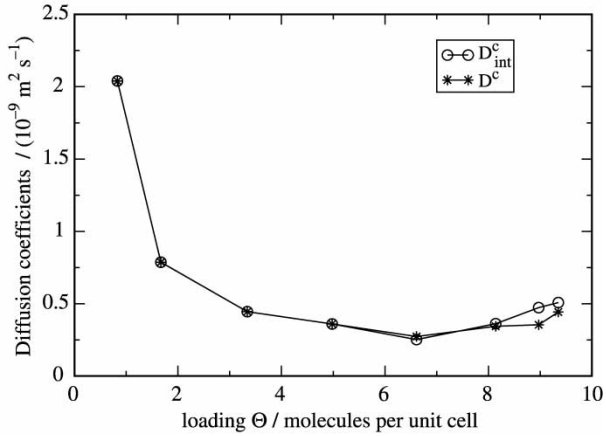

FIGURE 8 Comparison between the global (*) and intracrystalline (○) corrected Fick's diffusion coefficients of *n*-butane at 300 K as a function of the loading of the zeolite calculated from the simulations corresponding to the initial cases 2–4, 8, 9, 11–13 of Table II. The two corrected diffusion coefficients (D^{c} and D^{c}_{int}) are identical up to 8.3 molecules per unit cell (in the statistical uncertainty). For loadings higher than 8.3 molecules per unit cell the intracrystalline diffusion coefficients are higher. This can be associated with the adsorption on the external surface which have slower kinetics than the intracrystalline one. Generally, except for higher loadings one observes a general decrease of the corrected diffusion coefficients; this behavior agrees with previous results from simulations and experiments [7,9,25].

The corrected diffusion coefficients (D^{c} and D^{c}_{int}) shown on Fig. 8 are lower than the Fickian ones. The behavior of the former consist of a rapid decrease up to approximately 6 molecules per unit cell and then it starts to increase very slowly. This behavior corroborates previous results [6,9,7].

To study the effect of the initial gas density we simulated the kinetics with different simulation box dimensions and by having always 100 molecules (cases 5, 6 and 7 of Table II). In Fig. 9, we give the results obtained for these studies and these are represented by the uptake curves. The related diffusion coefficients are given in Table III. Figure 9 shows the effect of the simulation box size on the kinetics. Although the initial conditions are very different, the equilibrium states are nearly the same. Assuming, as it is generally admitted, that the time for each molecule to cross the gas is negligible compared to the whole kinetics and that there is no barrier at the external surface, we would expect the kinetics to be the same. However, we observe a dilution effect; increasing the volume of the gas density decreases the kinetics. This seems to indicate that under these particular conditions the limiting step of the adsorption kinetics is not the intracrystalline diffusion of the adsorbed molecules but the transport of the molecules in the gas. This unexpected behavior will be the subject of an extensive analysis in a forthcoming article. Moreover, for the highest initial gas density studied, the kinetics seems to be principally limited by intracrystalline diffusion and with a partial influence from the external surface. This has been confirmed by the simulation with 250 molecules (case 1 of Table II). Therefore, we may expect that by increasing the size of the aggregate and thus by decreasing

the surface–volume ratio will imply a reduction of the dilution effect.

CONCLUSIONS

We have shown in this work that the transient nonequilibrium molecular dynamics (TNEMD) can be used successfully to describe the adsorption of the *n*-butane on a silicate aggregate, with external surfaces, at constant volume. These simulation conditions are close to those used to study experimentally the same phenomena by manometry. The advantage of this simulation approach (TNEMD) is that it allows us to study the transfer of matter from the gas phase till the micropores and also gives information about the equilibrium state.

The isotherm obtained at 300 K agrees with previous works and we identified, at equilibrium, five energetic sites on the aggregate. Three sites are situated inside the micropore, as expected; straight, zig-zag channels and their intersections (with interaction energies respectively: −61, −64, −55 kJ/mol) and two additional ones are located at the external surfaces; one on the flat zones (−14 kJ/mol) and the second one at the bottom of half channels (−30 kJ/mol). At high loadings, close to the saturation, the last two sites are occupied which is not the case at low loadings (below 8.3 molecules per unit cell). For the simulated kinetics we obtained that above a certain volume, the limiting step of the adsorption kinetics seems to be the crossing of the gas phase by the molecule and not the intracrystalline diffusion. This last issue will be analyzed in more detail in a forthcoming article where we will use bigger silicalite clusters (220 000 Å^3). Finally, beside the fact that the approach used here reproduces satisfactorily previous diffusion coefficients obtained experimentally and by other simulations, the method seems to be well situated to analyze the experimental results obtained by manometry since it allows to mimic similar experimental conditions where the gas density is varied.

References

[1] Flanigen, E.M. (2001) "Zeolites and molecular sieves. An historical perspective", In: van Bekkum, H.V., Flanigen, E.M., Jacobs, P.A. and Jansen, J.C., eds, *Introduction to Zeolite Science and Practice*, Studies in surface science and catalysis (Elsevier) **137**, p 11.

[2] McCusker, L.B. and Baerlocher, C. (2001) "Zeolite structure", In: van Bekkum, H.V., Flanigen, E.M., Jacobs, P.A. and Jansen, J.C., eds, *Introduction to Zeolite Science and Practice*, Studies in surface science and catalysis (Elsevier) **137**, p 37.

[3] Maxwell, I.E. and Stork, W.H.J. (2001) "Hydrocarbon processing with zeolites", In: van Bekkum, H.V., Flanigen, E.M., Jacobs, P.A. and Jansen, J.C., eds, *Introduction to Zeolite Science and Practice*, Studies in surface science and catalysis (Elsevier) **137**, p 747.

[4] Martens, J.A. and Jacobs, P.A. (2001) "Introduction to acid catalysis with zeolites in hydrocarbon reactions", In: van Bekkum, H.V., Flanigen, E.M., Jacobs, P.A. and Jansen, J.C., eds, *Introduction to Zeolite Science and Practice*, Studies in surface science and catalysis (Elsevier) **137**, p 633.

[5] Paschek, D. and Krishna, R. (2001) "Inter-relation between self- and jump-diffusivities in zeolites", *Chem. Phys. Lett.* **333**, 278.

[6] Ruthven, D.A. and Post, M.F.M. (2001) "Diffusion in zeolite molecular sieves", In: van Bekkum, H.V., Flanigen, E.M., Jacobs, P.A. and Jansen, J.C., eds, *Introduction to Zeolite Science and Practice*, Studies in surface science and catalysis (Elsevier) **137**, p 525.

[7] Jobic, H. (2000) "Diffusion of linear and branched alkanes in ZSM-5. A quasi-elastic neutron scattering study", *J. Mol. Catal. A: Chem.* **158**, 135.

[8] van Santen, R.A., van de Graaf, B. and Smit, B. (2001) "Introduction to zeolite theory and modelling", In: van Bekkum, H.V., Flanigen, E.M., Jacobs, P.A. and Jansen, J.C., eds, *Introduction to Zeolite Science and Practice*, Studies in surface science and catalysis (Elsevier) **137**, p 419.

[9] Leroy, F., Rousseau, B. and Fuchs, A.H. (2004) "Self-diffusion of *n*-alkanes in silicalite using molecular dynamics simulation: a comparison between rigid and flexible frameworks", *Phys. Chem. Chem. Phys.* **6**, 775.

[10] Vlugt, T.J.H., Dellago, C. and Smit, B. (2000) "Diffusion of isobutane in silicalite studied by transition path sampling", *J. Chem. Phys.* **113**, 8791.

[11] Kobayashi, Y., Takami, S., Kubo, M. and Miyamoto, A. (2002) "Non-equilibrium molecular simulation studies on gas separation by microporous membranes using dual ensemble molecular simulation techniques", *Fluid Phase Eq.* **194–197**, 319.

[12] Furukawa, S., McCabe, C., Nitta, T. and Cummings, P.T. (2002) "Non-equilibrium molecular dynamics simulation study of the behavior of hydrocarbon-isomers in silicalite", *Fluid Phase Eq.* **194–197**, 309.

[13] de Groot, S.R. and Mazur, P. (1984) *Non-equilibrium Thermodynamics* (Dover Publications Inc., New York).

[14] Ermoshin, V.A., Smirnov, K.S. and Bougeard, D. (1996) "*Ab initio* generalized valence force field for zeolite modelling. 1. Siliceous zeolites", *Chem. Phys.* **202**, 53.

[15] van Koningsveld, H., van Bekkum, H. and Jansen, J.C. (1987) "On the location and disorder of the tetrapropylammonium (TPA) ion in zeolite ZSM-5 with improved framework accuracy", *Acta Cryst.* **B43**, 127.

[16] Ryckaert, J.P. and Bellemans, A. (1978) "Molecular dynamics of liquid alkanes", *Faraday Disc. Chem. Soc.* **66**, 95.

[17] Vlugt, T.J.H., Krishna, R. and Smit, B. (1999) "Molecular simulations of adsorption isotherms for linear and branched alkanes and their mixture in silicalite", *J. Phys. Chem. B* **103**, 1102.

[18] Smirnov, K.S. and van de Graaf, B. (1996) "Study of methane adsorption in MFI and MEL zeolites by combination of the electronegativity equalization method and molecular dynamics", *J. Chem. Soc. Faraday Trans.* **92**, 2475.

[19] Rees, L.V.C. and Shen, D. (2001) "Adsorption of gases in zeolite molecular sieves", In: van Bekkum, H.V., Flanigen, E.M., Jacobs, P.A. and Jansen, J.C., eds, *Introduction to Zeolite Science and Practice*, Studies in surface science and catalysis (Elsevier) **137**, p 579.

[20] Allen, M.P. and Tildesley, D.J. (1987) *Computer simulation of liquids* (Oxford University Press, Oxford).

[21] Evans, D.J. and Morriss, G.P. (1990) *Statistical Mechanics of Nonequilibrium Liquids* (Academic Press, London).

[22] Krishna, R. and Paschek, D. (2001) "Molecular simulations of adsorption and siting of light alkanes in silicalite-1", *Phys. Chem. Chem. Phys.* **3**, 453.

[23] Sun, M.S., Shah, D.B., Xu, H.H. and Talu, O. (1998) "Adsorption equilibria of C_1 to C_4 alkanes, CO_2, and SF_6 on silicalite", *J. Phys. Chem. B* **102**, 1466.

[24] Crank, J. (1956) *The Mathematics of Diffusion* (Oxford University Press, London).

[25] Millot, B., Méthivier, A., Jobic, H., Moueddeb, H. and Dalmon, J.A. (2000) "Permeation of linear and branched alkanes in ZSM-5 supported membranes", *Microp. Mesop. Mat.* **38**, 85.